19 Mar 2015

Microfracture and Surfactant Impact on Linear Cocurrent Brine Imbibition in Gas-saturated Shale

Yongpeng Sun

Baojun Bai
Missouri University of Science and Technology, baib@mst.edu

Mingzhen Wei
Missouri University of Science and Technology, weim@mst.edu

Recommended Citation

Y. Sun et al., "Microfracture and Surfactant Impact on Linear Cocurrent Brine Imbibition in Gas-saturated Shale," *Energy and Fuels*, vol. 29, no. 3, pp. 1438 - 1446, American Chemical Society, Mar 2015.
The definitive version is available at https://doi.org/10.1021/ef5025559

energy&fuels Article
pubs.acs.org/EF

Microfracture and Surfactant Impact on Linear Cocurrent Brine Imbibition in Gas-Saturated Shale

Yongpeng Sun,[†,‡] Baojun Bai,*[,†] and Mingzhen Wei[†]

[†]Department of Geosciences and Geological and Petroleum Engineering, Missouri University of Science and Technology, Rolla, Missouri 65409, United States

[‡]School of Petroleum Engineering, China University of Petroleum (East China), Qingdao, Shandong 257061, China

ABSTRACT: During and after hydraulic fracturing, fluid−shale interaction has a prominent impact on liquid retention and thus on gas phase permeability and gas productivity. By providing a low surface tension or wettability alteration, surfactants are widely used to decrease liquid retention after fracturing. To evaluate the liquid intake of a rock sample, an imbibition experiment is commonly used, especially when it is treated by a surfactant. However, conventional imbibition experiments with gas shale could not quantitate the imbibition behaviors as it does with conventional rocks because of the low porosity and extremely low permeability of gas shale. In this paper, a comprehensive experimental method was successfully developed to study the liquid imbibition in shale samples. Bulk shale easily fell apart during imbibition experiments. However, samples prepared with the coating method decribed herein remained intact except for fractures generated in them during the first imbibition. On each imbibition curve with imbibed mass as a function of time, two imbibition rates were identified: first imbibition rate at early stage and the second imbibition rate at later stage. For each sample, the imbibition experiment was performed three times. The sample was treated by surfactant between the second and the third imbibitions. All fractures were generated during the first imbibition. The characteristics of these fractures, such as quantity and distribution, are described in detail. In order to avoid the microfracture impact, the second and the third imbibition data were used to study the surfactant impact on the liquid intake in shale. The surfactant worked well to reduce the mass gain in shale. The effects of the existence of fractures, sample length, surfactant concentration, and treatment methods on the first and second imbibition rates were all studied in detail.

1. INTRODUCTION

Shale gas has been proven to be economically viable through horizontal drilling and hydraulic fracturing. This technology generates complex fracture networks in the target formation and exposes the shale matrix through numerous micrometer-sized fractures. Apart from these microfractures, the shale matrix usually has extremely low permeability and small sized pores.[1] Shale is composed of organic matter and a nonorganic matrix. Organic matter is hydrophobic, while the nonorganic matrix and natural fractures are more likely hydrophilic.[2] Therefore, in a shale gas reservoir, shale rock is generally fractional wet or mixed-wet.[3−5] During slickwater fracturing, the aqueous saturation is suspected to be limited in the nonorganic framework.[2] Because the organic matter usually occupies a very small fraction of the rock (usually <5%),[6] the contact angle measurement indicates that most shale rock behaves more like water-wet.[1,7]

After hydraulic fracturing with a water-based liquid, the water-wet matrix usually causes high water saturation and fluid retention, thus damaging gas-phase permeability[8−10] and impairing gas productivity. Lab experiments indicate that the water saturation near wellbore could be as high as 80%.[11] After 1000 days of drainage, it is still 60%. Some liquid in micropores may never be produced. Therefore, fluid retention is one of the major concerns for successful hydraulic fracturing operation in shale gas reservoirs. After fracturing, the fluid flow back could be as little as 5% in Haynesville shale to as much as 50% in areas of Barnett and Marcellus shale.[12] For those water-wet shale gas reservoirs stimulated by slickwater fracturing, liquid imbibition under capillary forces is the major reason for the fluid retention in pore spaces.[13] Unlike oil reservoirs under water drive, liquid imbibition is considered to be a negative factor in the recovery of shale gas reservoirs.[14,15]

Two types of liquid imbibition are usually studied on gas saturated shale: cocurrent imbibition, in which wetting and nonwetting phases flow in the same direction, and counter-current imbibition, in which the wetting phase imbibes into the sample, displacing the nonwetting phase out of the sample. Because of the low porosity and extremely low permeability of shale,[16] conventional imbibition experiments with Amott-USBM method usually take a long time, and the amount of liquid intrusion is difficult to observe. Recently, with digital sensors, such as a digital balance, the amount of liquid imbibed into shale samples can be recorded as a function of time.[17] For the microfractures in shale gas reservoir, the shale matrix near the fracture has one face open to fracturing liquid and the other face to reservoir gas during hydraulic fracturing. Therefore, cocurrent imbibition is widely used in this type of study. This method involves exposing one face of a shale sample to liquid and the other face to air and measuring the mass of liquid uptake over time.

However, during the imbibition experiments, liquid always introduces fractures in bulk shale, making them fall apart easily.[16,18,19] Shale is deposited in a layer-by-layer fashion and

Received: November 17, 2014
Revised: February 21, 2015
Published: February 23, 2015

DOI: 10.1021/ef5025559
Energy Fuels 2015, 29, 1438−1446

features high clay content. The bonding between each layer is usually not very strong. Therefore, the adsorption of water on the clay surface disintegrates the layers easily. Moreover, the wetted thin layer is very fragile. It almost cannot hold its integrity under any force, even gravity force. However, a coating method has been developed for cocurrent imbibition studies.[20,21] It confines fragile shale samples as it would be underground. The sealed coating around the sample by adhesives, such as epoxy, ensures one-dimensional liquid flow and prevents lateral liquid diffusion and evaporation around the sample. The flow convergence near the edge of the sample is also eliminated.

In order to minimize the liquid retention, the effects of capillary pressure, wettability, pore radius, and interfacial tension in gas reservoirs were investigated.[22] It was concluded that the best way to enhance the liquid load recovery would be wettability alteration. A surfactant provides a low surface tension and interfacial tension. It reduces capillary pressure and alters the rock wettability from water-wet to intermediate-wet or oil-wet,[23−25] thus reducing water retention in matrix.[26] With Berea sandstone soaked in surfactant,[20] the sample surface which is strong water-wet initially, could attain a contact angle of 120° with water drop and 60° with oil drop. The surface changes to oil-wet. Before surfactant treatment, this sample takes in 0.56 pore volume (PV) of water. However, after the treatment, it takes in only less than 0.05 PV. This altered wettability by surfactant achieves a prominent impact on the liquid intake in Berea sandstone.

However, surfactant impacts on liquid intake in gas shale are not clear. The present study investigates the imbibition behavior in gas shale impacted by fractures and surfactant. A coating and slicing method was developed to prepare shale samples. When liquid was introduced, the sample shape remained intact rather than falling apart; however, fractures were generated within the sample. Three cocurrent imbibitions were implemented for each sample. Microfractures were observed to generate only during the first imbibition. Microfracture characteristics such as quantity and distribution were described in detail. With the second and the third imbibitions, brine intake in shale was investigated to study the surfactant impact on imbibition behavior. Imbibition rates from experimental results were analyzed at various conditions. The factors that could impact imbibition rate, such as existence of fractures, sample length, surfactant concentration, and treatment method, were examined in detail. The amount of liquid intake was analyzed to illustrate the effectiveness of surfactant in reducing the liquid retention in shale. This study helps to reveal the mechanism behind high liquid loading in shale and the function of surfactant in reducing it.

2. EXPERIMENTAL SECTION

2.1. Shale Samples and Their Preparation. Marcellus gas shale samples from a depth of 2128 m were used in this study. Its porosity was measured with a helium porosimeter to be 3.43% on average. Bulk shale with a 4 in. diameter was used to prepare small samples with coating and cutting methods as follows:

(1) Dry cut one piece from the bulk rock. Cut it into a cubic shape, and polish each surface with 60 grit sandpaper;
(2) Measure the dimension of the samples, then vaporize water in an oven at a temperature over 100 °C for 24 h;
(3) Cut an acrylic tube into a designed length, and load the cubic rock in the center of the tube; fill the annular space with epoxy, and cool it for 24 h;
(4) Slice the rock into the desired length with the acrylic tube, and take out the epoxy-coated shale sample. Then polish the two faces with 60, 180, and 320 grit sandpaper in sequence.

A prepared sample is shown in Figure 1.

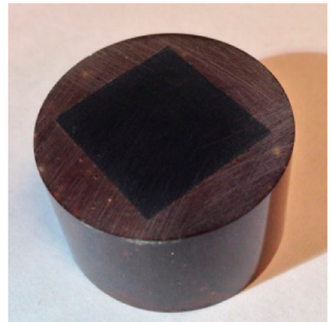

Figure 1. Sample with epoxy coating.

No liquid was introduced during sample preparation to prevent the clay from swelling and fracture generation. The dimensions of the samples prepared with this method are controllable. Their cross-sectional area and length could be measured accurately. Because it does not use 1 in. round core drilled from the bulk sample, it also results in less rock consumption. For one piece of the square shale sample coated in round shape, fracture generation during the imbibition experiment would not make the sample fall apart because of the confining epoxy, similar to what occurs underground. Because the sample has only two faces open, it can be used for cocurrent imbibition studies.

Because the hydrogeological data of Marcellus shale displays a wide range,[27] the samples used in this study were all sliced from the same 4 in. core. The detailed parameters are shown in Table 1. The thickness of some samples is around 5 mm ("short" samples), some are around 10 mm ("medium" samples), and some are around 15 mm ("long" samples).

Table 1. Shale Sample Parameters

sample no.	thickness (mm)	cross-sectional area (cm^2)
23	4.44	0.986
24	4.96	1.003
25	5.54	0.946
26	4.55	0.982
27	4.80	0.959
28	4.93	1.023
22	10.55	0.991
31	9.17	0.994
32	9.47	1.059
21	14.76	1.034
33	13.58	1.086

2.2. Fluids. *Clay Stabilizer.* 2% KCl was used throughout all imbibition experiments. A commercially available nonionic surfactant, commonly used in unconventional gas fracturing, was used in this study with three concentrations: 0.025, 0.05, and 0.1 vol %. Surface tensions were measured with the bubble method. The results are shown in Figure 2. To minimize the swelling of clay content during surfactant treatment, all surfactant solutions were prepared with 2% KCl.

2.3. Equipment. A conventional coreflooding and a self-build spontaneous cocurrent imbibition setup were used in this study, as presented in Figures 3 and 4. The coreflooding setup was used to inject the surfactant solution into the shale samples. Spontaneous imbibition setup was used to evaluate the liquid intake in shale samples before and after they were treated by surfactant solution.

DOI: 10.1021/ef5025559
Energy Fuels 2015, 29, 1438−1446

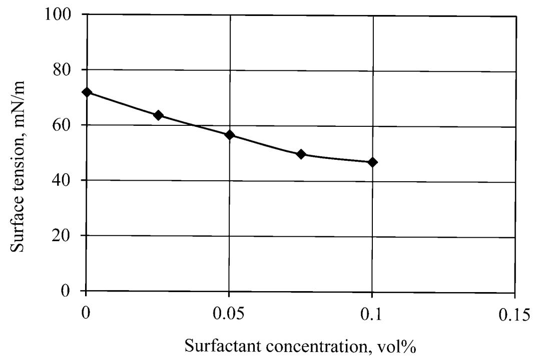

Figure 2. Surface tension measurement of surfactant.

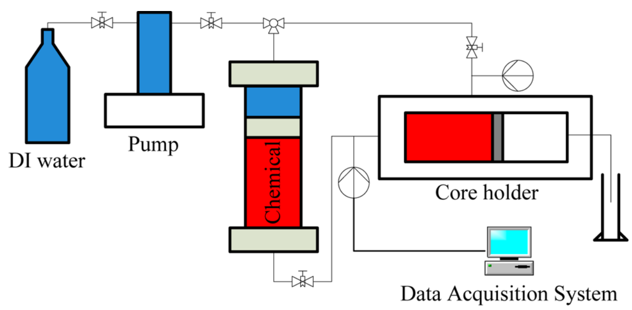

Figure 3. Coreflooding system.

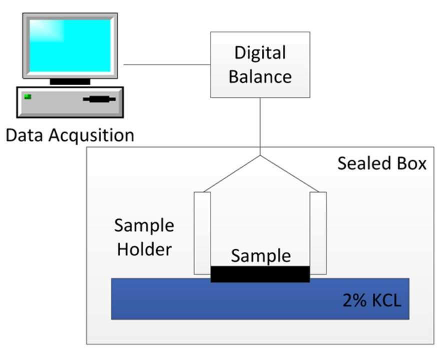

Figure 4. Spontaneous cocurrent imbibition system.

During the imbibition experiment, a sample was placed above the liquid horizontally. The sample was attached to a digital balanced (minimum reading of 0.0001g) through a sample holder. By gently and slowly adjusting the liquid upward, the sample started to contact the brine until its bottom was immersed 1 mm into the KCl solution. Then the capillary force was driving brine from the bottom in an upward direction. Therefore, the sample had one side facing air with the other side facing liquid, simulating the fracturing fluid transport from the fracture face into the matrix in the shale gas reservoir. The data acquisition software recorded the mass of water uptake as measured by the digital balance at certain time intervals (1 reading/5 s initially, then 1 reading/10 s). The entire setup was located in the basement of a building to minimize possible vibrations of the ground surface. The experiments were conducted at ambient conditions.

2.4. Procedure. Each shale sample was treated by the following procedure, as illustrated in Figure 5. The sample was first dried in an oven for 24 h to vaporize the water and moisture. Then the first imbibition was performed. When fluid is introduced to the shale sample during the first imbibition, because of the swelling of clay content, the force inside the sample will redistribute. When this force is accumulated to a value higher than the tensile strength of the shale sample, fractures will generate inside the sample, but no additional fractures were found after the second imbibition. After being dried in the oven for 24 h, the sample was treated by the surfactant: 50 PV flooding or soaked for 12 h. Then it was aged for 12 h and dried in oven for 24 h. The third imbibition was carried out. Each imbibition took from 2.5 to 7.5 h, depending on sample length. Each drying took 24 h in the oven.

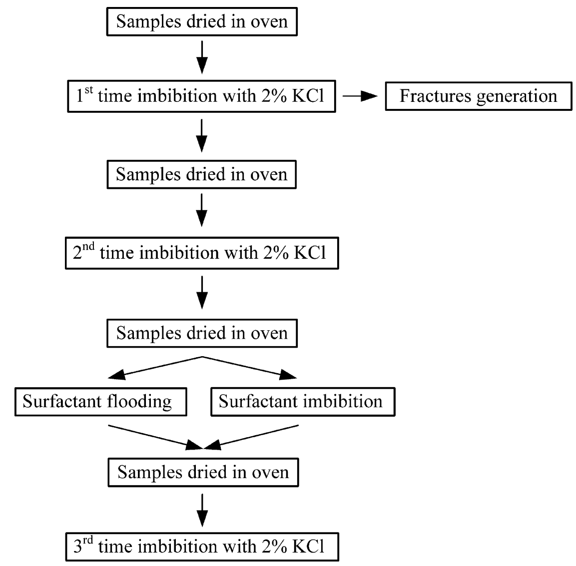

Figure 5. Flowchart of experimental procedure.

3. RESULTS AND DISCUSSION

With dozens of imbibition experiments, the imbibition curve is characterized first. Before surfactant treatment, the first and the second imbibitions are used to study the fracture impact on liquid intake. Then surfactant solution is applied to shale samples and the impact factors, such as sample length, surfactant concentration, and surfactant treatment method are examined in detail. The liquid intake during imbibition in samples is also discussed in detail.

3.1. Typical Imbibition Curve. It is well-known that the primary driving force for spontaneous cocurrent imbibition is capillary force and gravity force, and the relative influence between them is estimated by the following inverse bond number:[28−30]

$$N_B^{-1} = C\frac{\sigma\sqrt{\phi/k}}{\Delta\rho g H} \tag{1}$$

where N_B^{-1} is the inverse bond number. For the capillary tube model, $C = 0.4$. σ is the interfacial tension (N/m), ϕ the porosity (fraction), k the permeability (m^2; assumed to be 1 nD $= 10^{-21}$ m^2), $\Delta\rho$ the density difference between the two fluids (kg/m^3), g gravity (m/s^2), and H the height of the sample (m). N_B^{-1} is calculated to be 3 442 258, 1 721 129, and 1 147 419 for the 5, 10, and 15 mm thick samples, respectively. Because these inverse bond number are always larger than 5, capillary force is the primary driving force during imbibition.

A typical spontaneous cocurrent imbibition curve with 2% KCl solution in this gas shale is displayed in Figure 6. During the imbibition experiment, KCl travels from one pore to another via tubes connecting the two pores under the capillary pressure. The mass gain in the shale sample increases with time and is reflected through the digital balance.

There are two stages in the curve. At the early stage, the mass gain increases very fast as a function of time. After a while, it slows and maintains a second rate at the later stage. This

DOI: 10.1021/ef5025559
Energy Fuels 2015, 29, 1438−1446

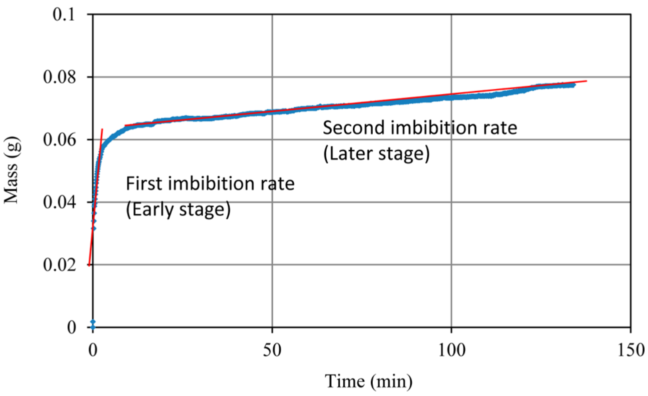

Figure 6. Typical imbibition curve.

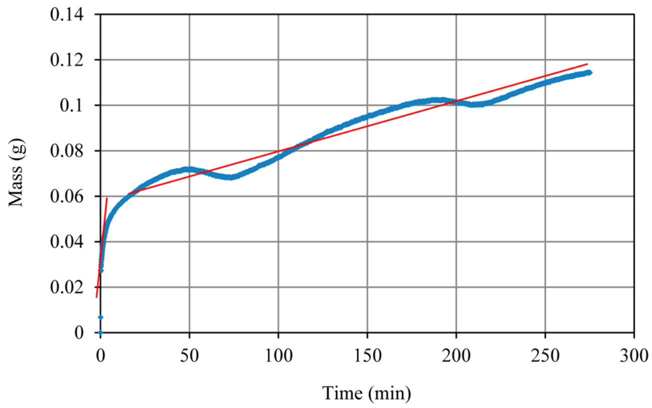

Figure 7. Imbibition curve with "pulse".

phenomenon was also observed by previous researchers on shale imbibition.[1,13,31] Two straight lines are placed on each stage to represent their slopes, which are also the imbibition rates. The line with high slope at the early stage is defined as the "first imbibition rate" here. The other line at the later stage is defined as the "second imbibition rate". The liquid intake rate is calculated as the slope of the linear regression line using the data covered by the red line, as in eq 2.

$$r = \frac{\sum (t - \bar{t})(m_g - \overline{m_g})}{\sum (t - \bar{t})^2} \quad (2)$$

where r is the slope of the curve, which is also the imbibition rate in g/min; t time in minutes; m_g the mass gain at corresponding time in grams; $\bar{t}$ the average time in minutes; and $\overline{m_g}$ the average mass gain in grams. With this quantified imbibition rate, the imbibition behavior was found to be comparable among different experimental conditions. Therefore, this imbibition rate is employed to study the impact of each factor in the following sections.

These two imbibition rates are significantly different from each other. The difference between them may be addressed by the relationship between capillary pressure and liquid saturation.[32] With the spontaneous liquid imbibing into the sample under capillary pressure, the increasing liquid saturation results in decreasing capillary pressure. Moreover, this is more obvious in low-permeability porous media.[8] These two rates were extensively found in all of the imbibition experiments in this study. However, among all of the 29 imbibition experiments, few of the curves are not as smooth, as illustrated in Figure 6. The mass gain in those shale samples has some vibrations as a function of time, as shown in Figure 7. This may be attributed to the sample heterogeneity, such as tortuosity, microfracture, and pore size distribution.[33] For those shale samples, there may be large pores or fractures far from the wetting front, and they are connected to the pore system through small pores, but they are not accessed at the early stage. At the later stage, when the wetting front encounters large pores or fractures through the small pores, the capillary pressure in the empty large pores will increase because of the decreased liquid saturation there. This may result in an increase of imbibition rate. With these pores or fractures filled by the wetting liquid, the capillary pressure decreases, and the liquid intake slows. Therefore, such a change of fluid intake in those samples behaves like a "pulse" and is reflected in the mass gain in the sample. For those few samples, this pulse behavior is minimized in the imbibition rate calculation with the experimental data.

3.2. Microfracture Impact on Imbibition Rate. To protect the samples from any influence or contamination such as fluid intrusion and clay swelling, each sample was carefully prepared to avoid any liquid contact before the imbibition experiment, except when it was cored from target zone underground as a 4 in. bulk core. After being coated and sliced with considerable attention, the sample surface was thoroughly examined. No fractures were found.

After the first KCl imbibition, the sample was taken out, and the extra liquid on the sample surface was gently cleaned. Because of the large surface area in clay content of shale, the sample surface usually dried out in few seconds and left few channels wetted by the imbibed brine. These channels existed in both sides. They were identified as fractures generated during the first imbibition. After the sample was dried in the oven, some fractures in the samples could still be observed with the naked eye. Most of these fractures extended across the sample surface and were distributed unevenly, as illustrated in Figure 8. Fracture width is in the micrometer range. For the

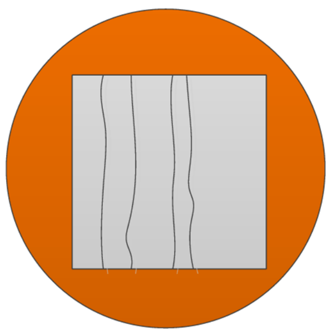

Figure 8. Typical fractures generated across the sample.

short samples, most of the microfractures extended throughout the sample length, but this did not happen to medium and long samples. This indicates that they could extend through sample length at least 5 mm depth. Around 5 fractures/cm^2 were found. Detailed information about fractures is listed in Table 2.

After the first KCl imbibition, the samples were dried in an oven and a second imbibition was carried out. Comparing the first and the second KCl imbibition, the first imbibition rate decreases to different extents, as shown in Figure 9a. The new fractures in the sample could be considered as larger pores, comparing with the original samples without fractures. Because

DOI: 10.1021/ef5025559
Energy Fuels 2015, 29, 1438−1446

Table 2. Statistics of the Fractures in Samples

sample no.	length (mm)	no. of fractures on both faces	fracture type
23	4.49	6	
24	4.96	7	3 throughout
25	5.49	4	2 throughout
26	4.59	6	3 throughout
27	4.84	7	1 throughout
28	4.96	6	1 throughout
22	10.64	6	
31	9.16	5	
32	9.44	6.5	
21	14.73	12	minor fracs
33	13.57	5	

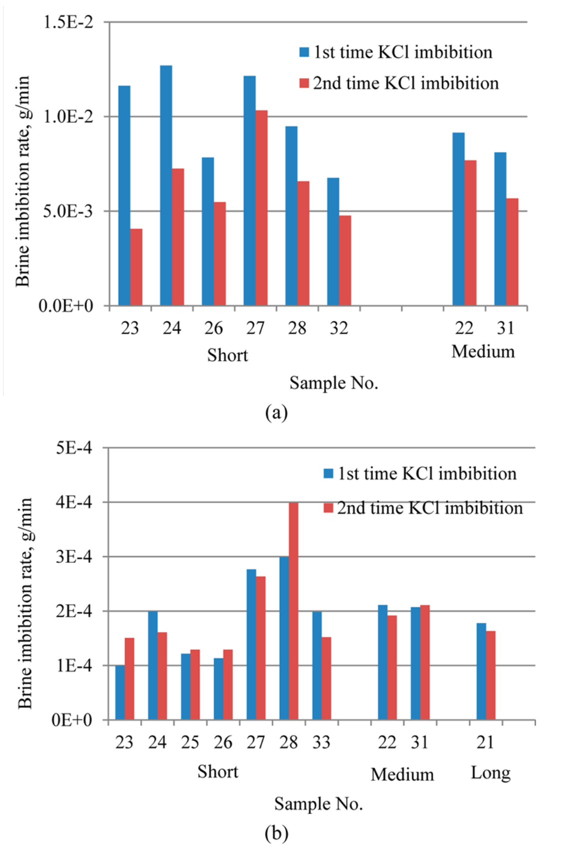

Figure 9. Fracture impact on first (a) and second (b) imbibition rate.

capillary pressure is in reverse relation with pore radius and brine solution is the wetting phase, the large pores result in a capillary pressure smaller than that before fractures are generated. Therefore, a lower imbibition rate is obtained in samples with fractures at the early stage.

However, the second imbibition rate, which is controlled by pores and fractures far from the wetting front, increases in some samples and decreases in others, as shown in Figure 9b. The variation in the second imbibition rate can be ascribed to the sample heterogeneity, such as tortuosity and pore size distribution, especially for the new pore space created by fractures.

After the second KCl imbibition, no more fractures were observed. Therefore, for a quantificational analysis of shale imbibition, such as imbibition rate impacted by introduced fluid and the liquid intake in shale, two imbibitions is suggested before further study to avoid the impact caused by fracture generation. In this study, the second and the third imbibition data are used for the analysis of surfactant impact on the spontaneous cocurrent imbibition in shale.

3.3. Sample Length Impact on Imbibition Rate after Surfactant Flooding.

After the second imbibition, surfactant was flooded into samples of different lengths. The length referred to here is the vertical length along the imbibition direction. After the sample was dried in an oven for 24 h, the third imbibition was conducted. No more fractures were found on the surface of the samples. Because of the adsorption of surfactant in the shale sample, the pore surface was modified after the sample was dried in the oven, resulting in different imbibition behavior. The imbibition rates from the second and the third imbibition curves were used to compare the surfactant impact on shale imbibition, as shown in Figure 10.

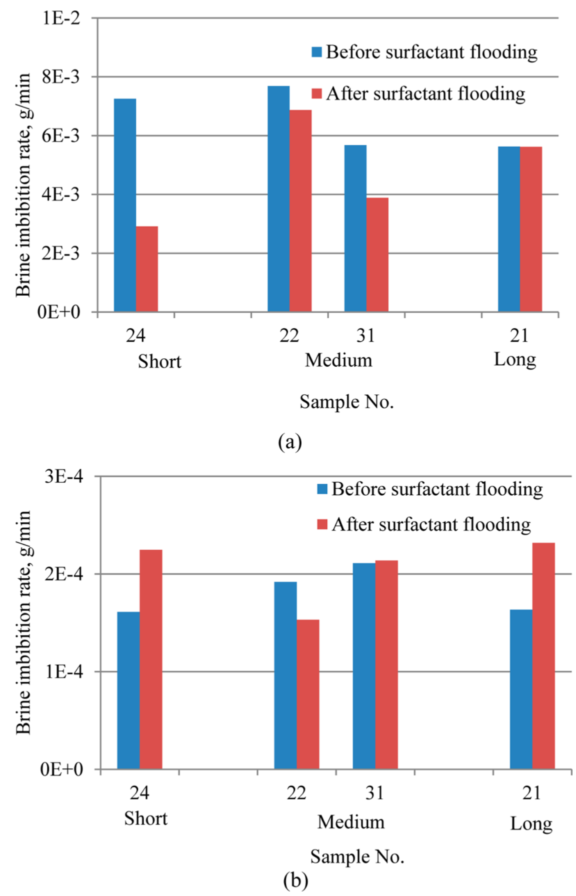

Figure 10. Sample length impact on first (a) and second (b) imbibition rate after surfactant flooding.

For the first imbibition rate, short samples get the most reduction. After surfactant flooding, short samples show a sharp decrease in the first imbibition rate, medium samples decrease a little, and long samples show almost no change. This may be explained by the accessible volume of surfactant flooding in shale. During surfactant flooding, a certain amount of surfactant, 50 PV, was flooded into each shale sample. In short samples, the surfactant could have a very high capacity to access most of the pore space. In medium and long samples, the pores are elongated and connected as a complex pore network system. With the fluid going deeper, it follows the preferential conduit instead of most of the pore space as in short samples. Therefore, under surfactant flooding, the sweep efficiency is

DOI: 10.1021/ef5025559
Energy Fuels 2015, 29, 1438−1446

much higher in short samples than that in medium and long samples, resulting in better wettability alteration.

However, for the second imbibition rate, samples with different lengths do not exhibit a consistent trend. This may be attributed to the pore size distribution deep in the sample matrix; in particular, they have different lengths. The variation of the imbibition rates was compared and is shown in Table 3.

Table 3. Imbibition Rates Impacted by Sample Length after Surfactant Treatment[a]

sample no.	sample length (mm)	change of the first imbibition rate (%)	change of the second imbibition rate (%)
24	4.96 (short)	59.8	28.3
22	10.55 (medium)	10.6	−25.3
31	9.17 (medium)	31.5	1.2
21	14.76 (long)	0.1	29.5

[a]Positive, imbibition rate increases; negative, imbibition rate decreases.

3.4. Surfactant Concentration Impact on Imbibition Rate. Following the second KCl imbibition and oven drying, the short samples were flooded with surfactant at three concentrations: 0.1, 0.05, and 0.025 vol %, respectively. After the samples were dried in the oven again, the third KCl imbibition was performed.

When the curves are compared with the curves before surfactant treatment, the higher the surfactant concentration, the more the first imbibition rate decreases, as displayed in Figure 11a. During surfactant flooding, with the same amount

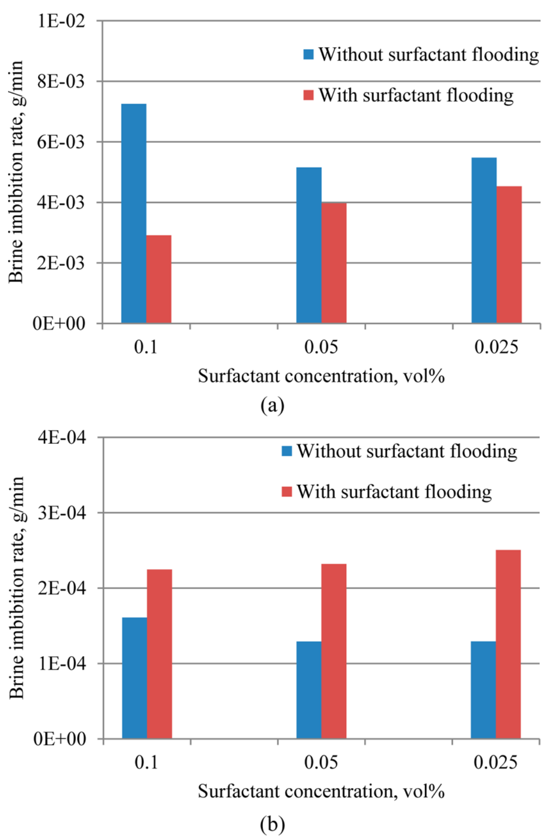

Figure 11. Surfactant concentration impact on first (a) and second (b) imbibition rate.

(50 PV) of surfactant injection, high-concentration surfactant solution results in better wettability alteration and thus lower imbibition rate.

However, the second imbibition rates are all higher than that before surfactant treatment, as shown in Figure 11b. The reason may be attributed to the relationship between capillary pressure and liquid saturation.[32] At the early stage of imbibition, the water-wet pore network before surfactant treatment attains liquid saturation higher than that after surfactant flooding. At the later stage of imbibition, this high liquid saturation before surfactant flooding would then result in low capillary pressure and thus smaller imbibition rate, compared with that after surfactant treatment.

Surfactant concentration also shows an impact on the second imbibition rate. The lower the surfactant concentration, the greater the increase of the second imbibition rate, as shown in Table 4. After surfactant flooding and dehydration in the oven,

Table 4. Imbibition Rates Impacted by Surfactant Concentration[a]

surfactant concentration (vol %)	change of the first imbibition rate (%)	change of the second imbibition rate (%)
0.1	−59.8	39.5
0.05	−22.9	79.5
0.025	−19.4	93.7

[a]Positive, imbibition rate increases; negative, imbibition rate decreases.

the sample treated with high concentration of surfactant had the maximum surfactant residual and correspondingly the smallest capillary pressure and imbibition rate among the three concentrations solutions.

Therefore, surfactant concentration has a positive impact on brine imbibition rate. High surfactant concentration achieves maximum reduction in the first imbibition rate at the early stage and the least increase in the second imbibition rate at the later stage. The contact angle on the shale surface was measured with a brine drop imaging method, as illustrated in Figure 12.

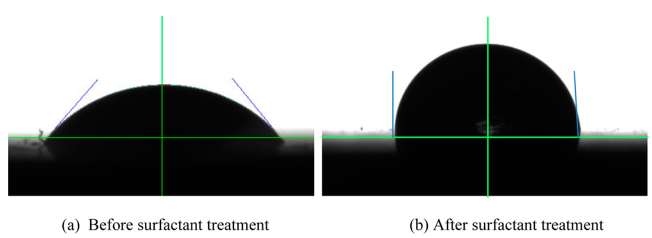

Figure 12. Contact angle on sample 26 with brine drop.

The contact angle is 49.9° before surfactant treatment and 97° after the treatment with 0.025% solution. The surface wettability is altered from water-wet to intermediate-wet, thus resulting in smaller water imbibition at the early stage.

3.5. Imbibition Rate Impacted by Different Surfactant Treatment Methods. All the imbibition data mentioned above were treated by surfactant flooding. During and after hydraulic fracturing, surfactant may be transported in the pore system under spontaneous cocurrent imbibition in the deep matrix. This could be represented by cocurrent surfactant imbibition into shale sample at no pressure drop. With one face of the short sample, SH27, contacted with 0.1 vol % surfactant solution and the other face open to air, imbibition was conducted for 12 h. Then the sample was dried in an oven and the third KCl imbibition was conducted.

The first imbibition rate decreases after the sample is treated with surfactant all at 0.025%, as displayed in Figure 13a.

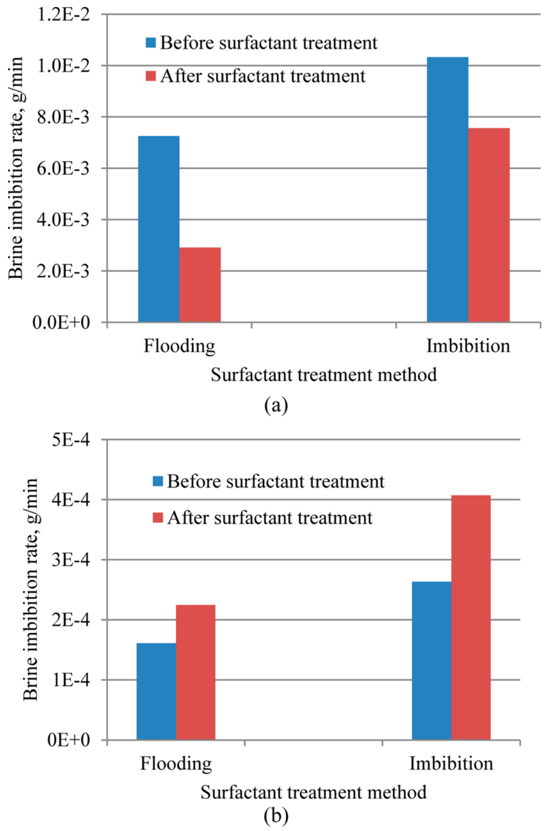

Figure 13. First (a) and second (b) imbibition rate impacted by different surfactant treatments.

Moreover, it decreases much more under surfactant flooding than imbibition. Surfactant flooding could realize higher surfactant saturation compared with that under surfactant imbibition, thus resulting in lower capillary pressure and smaller imbibition rate.

The second imbibition rates all increase compared with that before surfactant treatment, as shown in Figure 13b. The sample treated with surfactant flooding gains less than that by surfactant imbibition, as shown in Table 5. The reason is similar to that explained in section 3.4. The results from surfactant imbibition are quite similar to those from surfactant flooding at a lower concentration.

3.6. Total Liquid Intake. The conventional weighting method to estimate the liquid intake does not work well in shale imbibition studies, especially with small shale samples. Because shale has a relatively high portion of clay, the clay contents have very large surface area. Liquid evaporation from the shale surface is very fast, and this was observed in our study. Once extra liquid is gently wiped from the contact side, the remaining liquid in the surface pores would vaporize in a few seconds, leaving only water in the microfractures. Moreover, weighing the sample in a balance usually takes several seconds to stabilize then display reading. This fast liquid vaporization during weighing would introduce errors. In this study, the real-time mass gain in the sample is used to describe the liquid intake after imbibition. It is adopted from the last reading minus the first reading from the data acquisition system. Liquid evaporation is minimized because the sample is not removed from the sealed chamber.

Table 5. Imbibition Rate Impacted by Surfactant Treatment Method[a]

sample no.	surfactant treatment method	change of the first imbibition rate (%)	change of the second imbibition rate (%)
24	flooding	−59.8	39.5
27	imbibition	−26.8	54.5

[a]Positive, imbibition rate increases; negative, imbibition rate decreases.

Mass gain is used to describe the liquid imbibed into shale samples. It is the mass of the liquid intake in a sample over the sample's initial dry mass. Because of shale composition properties and sedimentary conditions, microfractures are easy to generate once liquid is introduced. After the first imbibition, the sample pore system contains not only the original pore space in the matrix, but also the introduced microfracture space.[19] Conventional terms based on initial sample porosity used to describe the liquid intake would not be accurate, such as liquid saturation, pore volume, and gas recovery. Because of the presence of microfractures, the liquid intake after imbibition in shale could be over 1 PV.[18] Mass gain in percentage then can be utilized in shale imbibition studies. With brine or water imbibition in shale samples, the mass gain is usually over 1%.[13,19,34] Sometimes, it could be over 5%.[18] This percentage is related to the sample's petrophysical properties, such as composition, porosity, and fracture generation.

In this study, in order that the liquid intake in different samples could be compared, the same imbibition strength between different samples was used. Imbibition time was controlled according to sample length: 1 mm length = 30 min imbibition. On the basis of our preliminary imbibition study, this imbibition strength is sufficient for the second imbibition rate at the later stage to maintain over 50% of the whole imbibition time, and the imbibition curves at the later stage are found to be pretty straight. With the same imbibition strength, the mass gain in different samples is listed in Table 6. After surfactant flooding, the liquid intake in all these samples is decreased. This is primarily attributed to the decreased surface tension and wettability alteration by the introduced surfactant.

Table 6. Mass Gain in Sample before and after Surfactant Flooding

sample length	sample no.	thickness (mm)	surfactant concentration (%)	mass gain during second imbibition (%)	mass gain during third imbibition (%)
short	SH24	4.96	0.1	6.19	3.30
	SH25	5.54	0.05	5.35	4.53
	SH26	4.55	0.025	6.28	4.36
medium	SH22	10.55	0.1	4.87	4.82
	SH31	9.17	0.1	4.82	3.88

Before the surfactant is applied, medium length samples acquire less mass gain than the short samples. However, the difference in mass gain is not obvious as a function of sample length after surfactant flooding. This change in mass gain impacted by the introduction of surfactant is displayed in

DOI: 10.1021/ef5025559
Energy Fuels 2015, 29, 1438−1446

Figure 14. Compared with the liquid intake before surfactant treatment, the mass gain decreases on average 30.9% in short

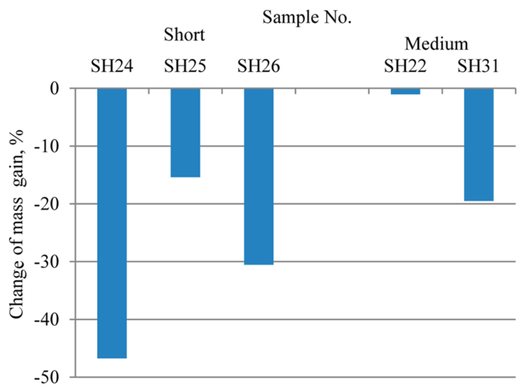

Figure 14. Change in sample mass gain after surfactant flooding.

samples and 10.3% in medium samples. In the short samples, because of the extension of microfractures throughout the sample length, the surfactant had much more capacity to come in contact with more matrix in depth through the fracture face. However, for the medium length samples, the fractures did not extend throughout the sample length. The sweep efficiency by surfactant was limited compared with that in the short samples. However, this change in mass gain did not show a consistent trend with concentration. This may be attributed to the samples' heterogeneity.

4. SUMMARY AND CONCLUSIONS

The following summary and conclusions may be drawn according to our present study:

(1) A comprehensive experimental method was developed to study the liquid intake with cocurrent imbibition method. Imbibition rate was used to describe the liquid intake in shale as a function of time. The first imbibition rate at the early stage is much higher than the second imbibition rate at the later stage.

(2) Microfractures were generated only during the first imbibition. They extended through sample length at least 5 mm depth and existed at around 5 fractures/cm^2. The existence of fractures in samples decreases the first imbibition rate.

(3) Surfactant only works to reduce the first imbibition rate. However, the second imbibition rate is increased after surfactant treatment. Short samples show maximum reduction in the first imbibition rate. High concentration surfactant gets the most reduction in the first imbibition rate, and the least increase in the second imbibition rate.

(4) When compared with the samples treated with surfactant imbibition, samples treated with surfactant flooding display better reduction in the first imbibition rate and the least increase in the second imbibition rate.

(5) The surfactant works to reduce the mass gain in shale. After surfactant flooding, the mass gain decreases an average of 30.9% in short samples and an average of 10.3% average in medium samples.

■ AUTHOR INFORMATION

Notes

The authors declare no competing financial interest.

■ ACKNOWLEDGMENTS

Funding for this project is provided by Research Partnership to Secure Energy for America (RPSEA) through the "Ultra-Deepwater and Unconventional Natural Gas and Other Petroleum Resources" program authorized by the U.S. Energy Policy Act of 2005. RPSEA (www.rpsea.org) is a nonprofit corporation whose mission is to provide a stewardship role in ensuring the focused research, development, and deployment of safe and environmentally responsible technology that can effectively deliver hydrocarbons from domestic resources to the citizens of the United States. RPSEA, operating as a consortium of premier U.S. energy research universities, industry, and independent research organizations, manages the program under a contract with the U.S. Department of Energy's National Energy Technology Laboratory. The authors also acknowledge the support from Baker Hughes and the China Scholarship Council.

■ REFERENCES

(1) Lakatos, I.; Bódi, T.; Lakatos-SzabC, J.; Szentes, G. *PVT Properties, Wettability and Capillary Forces in Unconventional Gas Reservoirs: Topics Rarely Visited*. Presented at SPE Reservoir Characterisation and Simulation Conference and Exhibition, Abu Dhabi, UAE 2011; Paper SPE 148157.

(2) Andrade Perdomo, J. F.; Civan, F.; Devegowda, D.; Sigal, R. F. *Accurate Simulation of Shale-Gas Reservoirs*. Presented at the SPE Annual Technical Conference and Exhibition, Florence, Italy, 2010; Paper SPE 135564 .

(3) Rimassa, S. M.; Howard, P. R.; Blow, K. A. *Optimizing Fracturing Fluids From Flowback Water*. Presented at the SPE Tight Gas Completions Conference, San Antonio, TX, 2009; Paper SPE 125336.

(4) Sondergeld, C. H.; Newsham, K. E.; Comisky, J. T.; Rice, M. C.; Rai, C. S. *Petrophysical Considerations in Evaluating and Producing Shale Gas Resources*. Presented at the SPE Unconventional Gas Conference, Pittsburgh, PA 2010; Paper SPE 131768.

(5) Sondergeld, C. H.; Ambrose, R. J.; Rai, C. S.; Moncrieff, J. *Micro-Structural Studies of Gas Shales*. Presented at the SPE Unconventional Gas Conference, Pittsburgh, PA 2010; Paper SPE 131771.

(6) Boyer, C.; Kieschnick, J.; Suarez-Rivera, R.; Lewis, R. E.; Waters, G. Producing gas from its source. *Oilfield Rev.* **2006**, *18* (3), 36−49.

(7) Andrade Perdomo, J. F.; Civan, F.; Devegowda, D.; Sigal, R. F. *Design and Examination of Requirements for a Rigorous Shale-Gas Reservoir Simulator Compared to Current Shale-Gas Simulator*. Presented at the North American Unconventional Gas Conference and Exhibition, The Woodlands, TX, 2011; Paper SPE 144401.

(8) Ford, W. G. F.; Penny, G. S.; Briscoe, J. E. Enhanced Water Recovery Improves Stimulation Results. *SPE Prod. Eng.* **1988**, 3 (4), 515−521.

(9) Gupta, D. V. S. *Unconventional Fracturing Fluids for Tight Gas Reservoirs*. Presented at the SPE Hydraulic Fracturing Technology Conference, The Woodlands, TX, 2009 Paper SPE 119424.

(10) Rickman, R. D.; Jaripatke, O. A. *Optimizing Micro-emulsion/Surfactant Packages for Shale and Tight Gas Reservoirs*. Presented at the SPE Deep Gas Conference and Exhibition, Manama, Bahrain, 2010; Paper SPE 131107.

(11) Bust, V. K.; Oletu, J. U.; Worthington, P. F. The challenges for carbonate petrophysics in petroleum resource estimation. *SPE Reservoir Eval. Eng.* **2011**, *14* (01), 25−34.

(12) King, G. E. *Hydraulic Fracturing 101: What Every Representative, Environmentalist, Regulator, Reporter, Investor, University Researcher, Neighbor and Engineer Should Know About Estimating Frac Risk and Improving Frac Performance in Unconventional Gas and Oil Wells*. Presented at the SPE Hydraulic Fracturing Technology Conference, The Woodlands, TX, 2012; Paper SPE 152596.

(13) Roychaudhuri, B.; Tsotsis, T. T.; Jessen, K. *An Experimental and Numerical Investigation of Spontaneous Imbibition in Gas Shales*.

Presented at the SPE Annual Technical Conference and Exhibition, Denver, CO ,2011; Paper SPE 147652.
(14) Kantzas, A.; Pow, M.; Allsopp, K.; Marentette, D. *Co-current and Counter-current Imbibition Analysis for Tight Fractured Carbonate Gas Reservoirs*. Presented at the Technical Meeting/Petroleum Conference of The South Saskatchewan Section, Regina, Canada ,1997; Paper PETSOC-97-181.
(15) Beattie, D.; Roberts, B. *Water Coning in Naturally Fractured Gas Reservoirs*. Presented at the SPE Gas Technology Symposium, Calgary, Alberta, Canada, 1996; Paper SPE 35643.
(16) Wang, D.; Butler, R.; Liu, H.; Ahmed, S. Flow-Rate Behavior and Imbibition in Shale. *SPE Reservoir Eval. Eng.* **2011**, *14* (04), 485−492.
(17) Li, K.; Horne, R. N. *Characterization of Spontaneous Water Imbibition into Gas-Saturated Rocks*. Presented at the SPE/AAPG Western Regional Meeting, Long Beach, CA 2000; Paper SPE 62552.
(18) Dehghanpour, H.; Zubair, M. H. A.; Chhabra, A.; Ullah, A. Liquid Intake of Organic Shales. *Energy Fuels* **2012**, *26* (9), 5750−5758.
(19) Dehghanpour, H.; Lan, Q.; Saeed, Y.; Fei, H.; Qi, Z. Spontaneous Imbibition of Brine and Oil in Gas Shales: Effect of Water Adsorption and Resulting Microfractures. *Energy Fuels* **2013**, *27* (6), 3039−3049.
(20) Li, K.; Abbas, F. Experimental Study of Wettability Alteration to Preferential Gas-Wetting in Porous Media and Its Effects. *SPE Reservoir Eval. Eng.* **2000**, *3* (2), 139−149.
(21) Hatiboglu, C. U.; Babadagli, T. Experimental and Visual Analysis of Diffusive Mass Transfer between Matrix and Fracture under Static Conditions. *J. Pet. Sci. Eng.* **2010**, *74* (1), 31−40.
(22) Penny, G. S.; Conway, M. W.; Briscoe, J. E. *Enhanced Load Water-Recovery Technique Improves Stimulation Results*. Presented at the SPE Annual Technical Conference and Exhibition, San Francisco, CA, 1983; Paper SPE 12149.
(23) Paktinat, J.; O'Neil, B. J.; Aften, C. W.; Hurd, M. D. *Critical Evaluation of High Brine Tolerant Additives Used in Shale Slick Water Fracs*. Presented at the SPE Production and Operations Symposium, Oklahoma City, OK, 2011; Paper SPE 141356.
(24) Gall, B.; Sattler, A.; Maloney, D.; Raible, C. *Permeability Damage to Natural Fractures Caused by Fracturing Fluid Polymers*. Presented at the SPE Rocky Mountain Regional Meeting, Casper, WY, 1988; Paper SPE 17542.
(25) Parekh, B.; Sharma, M. M. *Cleanup of Water Blocks in Depleted Low-Permeability Reservoirs*. Presented at the SPE Annual Technical Conference and Exhibition, Houston, TX, 2004; Paper SPE 89837.
(26) Adibhatla, B.; Mohanty, K.; Berger, P.; Lee, C. Effect of Surfactants on Wettability of Near-Wellbore Regions of Gas Reservoirs. *J. Pet. Sci. Eng.* **2006**, *52* (1), 227−236.
(27) Yu, M.; Lau, H.-C. *Production Technology Challenges of Tight and Shale Gas Production in China*. Presented at the International Petroleum Technology Conference, Beijing, China 2013; Paper SPE 17096.
(28) Standnes, D. C.; Nogaret, L. A. D.; Chen, H.-L.; Austad, T. An Evaluation of Spontaneous Imbibition of Water into Oil-Wet Carbonate Reservoir Cores Using a Nonionic and a Cationic Surfactant. *Energy Fuels* **2002**, *16* (6), 1557−1564.
(29) Rezaveisi, M.; Ayatollahi, S.; Rostami, B. Experimental Investigation of Matrix Wettability Effects on Water Imbibition in Fractured Artificial Porous Media. *J. Pet. Sci. Eng.* **2012**, *86*, 165−171.
(30) Kalaei, M. H.; Green, D. W.; Willhite, G. P. *Numerical Modeling of the Water Imbibition Process in Water-Wet Laboratory Cores*. Presented at the SPE Western Regional Meeting, Anaheim, CA, 2010; Paper SPE 132645.
(31) Roychaudhuri, B.; Tsotsis, T.; Jessen, K. An Experimental Investigation of Spontaneous Imbibition in Gas Shales. *J. Pet. Sci. Eng.* **2013**, *111*, 87−97.
(32) Tiab, D.; Donaldson, E. C. *Petrophysics: Theory and Practice of Measuring Reservoir Rock and Fluid Transport Properties*. Gulf Professional Publishing: Amsterdam, 2011.
(33) Bear, J.; Braester, C. On the Flow of Two Immiscible Fluids in Fractured Porous Media. *Dev. Soil. Sci.* **1972**, *2*, 177−202.
(34) Xu, M.; Dehghanpour, H. Advances in Understanding Wettability of Gas Shales. *Energy Fuels* **2014**, *28* (7), 4362−4375.

DOI: 10.1021/ef5025559
Energy Fuels 2015, 29, 1438−1446